Building Resiliency to Climate Change Uncertainty through Bioretention Design Modifications

R. Andrew Tirpak[1*], Jon M. Hathaway[2], Anahita Khojandi[3], Matthew Weathers[2], and Thomas H. Epps[4]
[1] Dept. of Food, Agricultural, and Biological Engineering, The Ohio State University, 590 Woody Hayes Dr., Columbus, OH, 43210, USA
[2] Dept. of Civil and Environmental Engineering, University of Tennessee, Knoxville, TN, USA
[3] Dept. of Industrial and Systems Engineering, University of Tennessee, Knoxville, TN, USA
[4] Craftwater Engineering, San Diego, CA, USA
*Corresponding author: tirpak.5@osu.edu

Abstract

Climate stationarity is a traditional assumption in the design of the urban drainage network, including green infrastructure practices such as bioretention cells. Predicted deviations from historic climate trends associated with global climate change introduce uncertainty in the ability of these systems to maintain service levels in the future. Climate change projections are made using output from coarse-scale general circulation models (GCMs), which can then be downscaled using regional climate models (RCMs) to provide predictions at a finer spatial resolution. However, all models contain sources of error and uncertainty, and predicted changes in future climate can be contradictory between models, requiring an approach that considers multiple projections. The performance of bioretention cells were modeled using USEPA's Storm Water Management Model (SWMM) to determine how design modifications could add resilience to these systems under future climate conditions projected for Knoxville, Tennessee, USA. Ten downscaled climate projections were acquired from the North American Coordinated Regional Downscaling Experiment program, and model bias was corrected using Kernel Density Distribution Mapping (KDDM). Bias-corrected climate projections were used to assess bioretention hydrologic function in future climate conditions. Several scenarios were evaluated using a probabilistic approach to determine the confidence with which design modifications could be implemented to maintain historic performance for both new and existing (retrofitted) bioretention cells. The largest deviations from current design (i.e., concurrently increasing ponding depths, thickness of media layer, media conductivity rates, and bioretention surface areas by 307%, 200%, 200%, and 300%, respectively, beyond current standards) resulted in the greatest improvements on historic performance with respect to annual volumes of infiltration and surface overflow, with all ten future climate scenarios across various soil types yielding increased infiltration and decreased surface overflow compared to historic conditions. However, lower performance was observed for more conservative design modifications; on average, between 13-82% and 77-100% of models fell below historic annual volumes of infiltration and surface overflow, respectively, when ponding zone depth, media layer thickness, and media conductivity were increased alone. Findings demonstrate that increasing bioretention surface area relative to the contributing catchment provides the greatest overall return on historic performance under future climate conditions and should be prioritized in locations with low *in situ* soil drainage rates. This study highlights the importance of considering local site conditions and management objectives when incorporating resiliency to climate change uncertainty into bioretention designs.

Keywords: Bioretention; climate change; hydrology; water balance; resiliency; SWMM

1.0 Introduction

For several decades, research has connected urbanization and land development to impacts on the hydrologic cycle and receiving water bodies (Leopold, 1968; Hollis, 1975; Klein, 1979; Arnold and Gibbons, 1996; Booth and Jackson, 1997; Walsh et al., 2005). Cities worldwide are employing green infrastructure (GI) techniques, referred to as stormwater control measures (SCMs), low impact development (LID), and water sensitive urban design (WSUD), to manage urban runoff. One of the most popular SCMs is the bioretention cell, which manages runoff volumes by promoting infiltration, temporary retention, and evapotranspiration, and removes pollutants via natural treatment mechanisms such as soil adsorption, filtration, and plant/microbial uptake (Davis et al., 2009). Many studies have demonstrated their ability to reduce runoff volumes and mitigate peak flow rates to levels that resemble pre-development hydrologic conditions (e.g., Brown and Hunt, 2011; DeBusk and Wynn, 2011; Winston et al., 2016).

Bioretention designs are commonly based on past climate conditions, where treatment objectives (e.g., retaining runoff from the 90th percentile storm on-site) derived from historic records are used to determine key parameters such as surface area. This relies on the assumption of climate stationarity, where such targets remain constant over time (Denault et al., 2006). However, climate change challenges this approach, threatening to overwhelm existing systems and risking diminished performance or operational failure (Denault et al., 2006; Berggren et al., 2012; Hathaway et al., 2014). There is widespread agreement that surface temperatures and extreme weather shifts will increase over the 21st century due to global climate change, though the magnitude of change is uncertain and dependent upon many factors, including anthropogenic emissions, human adaptation, technological advances, and natural climate variability (Berliner, 2003; IPCC, 2014). Given the operational lifespan of these systems (beyond 20-25 years), the functionality of presently installed SCMs in future climate conditions is under question (Zhang et al., 2019). Therefore, despite future climate uncertainties, there is a need to investigate methods to develop climate resilient bioretention designs which maintain performance under shifting hydrologic regimes (Rosenberg et al., 2010).

Climate change impact studies rely on future projections based on general circulation models (GCMs) (IPCC, 2014; Semadeni-Davis et al., 2008). Although GCMs generally simulate the same processes, all models approach the global system differently and contain variable sources of error, uncertainty, and sometimes contradictory projections (Semadeni-Davies, 2008); thus, research recommends the use of an array of GCMs to better understand potential future climate changes (Rosenberg et al., 2010; Zhang et al., 2019; Barah et al., 2020; Ramshani et al., 2020). Because the spatial scale of GCMs (on the order of hundreds of kilometers) is too coarse for the small catchments associated with urban hydrology (tens of kilometers or less), outputs from large-scale GCMs are often transformed for use in smaller-scale applications utilizing dynamic downscaling techniques such as regional climate models (RCMs) (Willems et al., 2012). However, because climate uncertainty is magnified at the regional scale, resulting systematic bias must be corrected via statistical downscaling methods prior to assessing local-scale climate impacts (Semadeni-Davies et al., 2008; Willems et al., 2012; Mearns et al., 2017).

Despite the limited availability of fine-scale climate projections, studies have investigated climate change impacts on bioretention performance using various techniques. A common approach is the delta change factor (DCF) method, where relative changes predicted by climate models are applied to an observed rainfall series to produce future precipitation projections (Anandhi et al., 2011). Numerous studies have modeled GI under future conditions by applying change factors to alter precipitation volume, intensity, and seasonal patterns (Semadeni-Davies et al., 2008; Olsson et al., 2009; Pyke et al., 2011; Moore et al., 2016). Despite its ease of use, the DCF method contains several disadvantages and may not fully consider all aspects of changing climate conditions that influence GI (e.g., event frequency, changes in antecedent conditions, etc.) (Anandhi et al., 2011).

Other studies have implemented different approaches to assess climate change impacts on GI performance. Zahmatkesh et al. (2014) analyzed historic rainfall patterns to develop hourly multipliers and disaggregate daily climate output from 134 GCMs into hourly rainfall projections for New York City. Zahmatkesh et al. (2015) investigated the effectiveness of LID under future climate using this methodology. Despite annual runoff volumes increasing by 48%, the authors observed a 41% decline in average annual runoff volumes and peak flow reductions of 8-13% in model scenarios where LID practices (porous pavement, rainwater harvesting, and bioretention cells) were implemented. Zhang et al. (2019) analyzed the reliability of WSUDs in Melbourne, Australia using an ensemble of eight GCMs. Using historical rainfall data and a multiplicative random cascade model (HiDRUS), 100 continuous rainfall projections were developed for each GCM at high spatial (1 km) and temporal (6-minute) resolutions. Results showed lower precipitation and longer dry periods in the future, with minimal impact on WSUD performance. Large variability was observed across the GCMs, and larger practices were recommended to account for this uncertainty and maintain future performance (Zhang et al., 2019). Wang et al. (2019a) used intensity-duration-frequency (IDF) curves to evaluate GI performance in a hypothetical catchment in Guangzhou, China using historical data and 11 GCMs under four representative concentration pathways (RCPs) (IPCC, 2014). Larger practices yielded increased runoff volume reductions, though performance improvements decreased with increasing GI surface area. Similarly, GI effectiveness decreased as storm sizes and return periods increased (Wang et al., 2019a).

Given the highly regional and uncertain nature of climate change impacts, and the limited research investigating its effects on bioretention, there is a critical need to examine the ability of these systems to maintain performance in future conditions. Further, there is a need to determine how bioretention design elements impact future performance such that regulatory agencies, stormwater engineers, and municipal officials can build climate resiliency into these systems.

The objective of this study was to investigate the impact of climate change on future bioretention performance and determine how design modifications and site conditions influence the climate resiliency of these systems. Using a probabilistic approach, bioretention hydrology under various climate change scenarios was compared to a baseline period to determine the design modifications required to achieve past performance under future climate conditions. While the study area was in the southeastern United States, this approach may be applicable to broader geographical regions, allowing the prioritization of specific design elements that enhance the resiliency of bioretention cells to climate change. Though studies have investigated climate change impacts on bioretention performance, to the authors' knowledge, no studies have addressed this research gap using such methodology.

2.0 Materials and Methods

2.1 Conceptual study location

The hypothetical study site was based on the climate of Knoxville, Tennessee, USA (35.9606°N, 83.9207°W, approximate elevation 270 m). The mean annual temperature in Knoxville is 16°C, while the mean annual precipitation is approximately 1215 mm (Tennessee

Climatological Service). The frequency and severity of extreme rainfall events are expected to increase across the southeastern United States under both lower and higher emissions scenarios in the future, posing risks to human health, frequent and prolonged drought, and increased spread of vector borne disease (USGCRP, 2018).

The hypothetical catchment represented an impervious surface common to urban areas (e.g., a paved parking lot) and consisted of a relatively flat, completely impervious, 0.4 ha area draining to a single bioretention cell. Three underlying soil types (ranging from clay to sandy loam) were modeled to capture the potential variability of climate change impacts on bioretention performance at locations with different soil characteristics. Observed climate data for the baseline period (2010-2014) was obtained from a weather station at the nearest airport (McGhee Tyson) and used to simulate historic performance.

2.2 Hydrological model

The USEPA Storm Water Management Model (SWMM) version 5.1 was used to assess bioretention hydrologic performance in this study (Rossman, 2015; Niazi et al., 2017). All runoff from the hypothetical catchment was routed to the bioretention cell; depression storage was not considered to simulate the complete connection of the catchment to the outlet. Infiltration was estimated using the Green-Ampt method, and dynamic wave flow routing was used in the models (Rossman, 2015). Evaporation was estimated from daily air temperatures using the Hargreaves method (Hargreaves and Samani, 1985; Rossman, 2015). Hourly rainfall from observed data (baseline period – 2010-2014) or climate change projections (future period – 2040-2044) were used as model inputs. Other parameters were determined from a review of literature and the characteristics of the simulated study location (Table 1). As the study focused on performance changes between the baseline and future climate conditions, as opposed to modeling a specific site, no calibration or verification of the models was performed (Wang et al., 2016).

Table 1: Summary of parameters of hypothetical catchment used in SWMM models.

Parameter	Description	Value
Area	Area of subcatchment (ha)	0.4
% Slope	Average surface slope (%)	1
% Imperv	Percent of impervious area (%)	100
N-Imperv	Manning's n for impervious area	0.01
% Zero	Percent of impervious area with no depression storage (%)	100
% Routed	Percent of runoff routed between sub-areas (%)	100

2.3 Model scenarios

The future performance of two model scenarios ("New Build" and "Retrofit") was simulated for a period from 2040-2044, representing the final five years of a 25-year service life for a bioretention cell constructed in 2020. The scenarios are described below:

- The New Build scenario represented a bioretention cell constructed in 2020. In this scenario, design components were modified beyond regulatory recommendations, and the resulting effects on performance under future climate was investigated (TDEC, 2014).
- The Retrofit scenario simulated modifications performed to an existing bioretention cell in 2020 in response to anticipated climate change. As more frequent and severe rain events are expected in the study area, increased instances of overflow could be expected to occur. In this scenario, the bioretention media layer thickness was incrementally decreased as the surface storage zone was deepened, representing the finite cross-section depth for the system. This was intended to simulate media removal from the practice to

increase surface storage depth, a measure that could theoretically be implemented in place of a full reconstruction.

2.4 Bioretention modeling and design configurations

Bioretention design parameters, such as practice size, media depth, and surface storage depth, were initially based on design criteria specified in the Tennessee Permanent Stormwater Management and Design Guidance Manual (TDEC, 2014). Initial designs were sized to capture runoff from a 25.4 mm storm in the surface storage zone. Components of the baseline design ("BASE") are shown in Table 2. Model parameters were incrementally adjusted from this design to form several configurations for the New Build and Retrofit scenarios (Table 3). Due to model limitations and a desire to quantify the performance implications following specific design modifications, factors which could reasonably impact bioretention performance over time (i.e., media porosity, field capacity, and clogging) remained unchanged from initial conditions in all simulations.

Table 2: Baseline bioretention design parameters (BASE).

Parameter	Description	Value	Source
Surface Layer			
Berm Height	Maximum depth water can pond in bowl (cm)	15	TDEC (2014)
Soil Layer			
Thickness	Soil layer thickness (cm)	61	TDEC (2014)
Porosity	Soil porosity (volume fraction)	0.44	Committee (2005)
Field Capacity	Soil field capacity (volume fraction)	0.09	Committee (2005)
Wilting Point	Soil wilting point (volume fraction)	0.04	Committee (2005)
Conductivity	Saturated hydraulic conductivity of soil (cm/hr)	5	Parameter adjusted in model scenarios
Conductivity Slope	Slope of log(conductivity)-soil moisture content curve	50	Rossman (2015)
Suction Head	Soil capillary suction (cm)	10	Brakensiek et al. (1981)
Storage Layer			
Thickness	Storage layer (soil) thickness (cm)	15	County (2008)
Void Ratio	Storage layer void ratio (voids/solids)	0.4	Miller (1978)
Seepage Rate	Rate of water seepage to native soil (mm/hr)	1.3	Parameter adjusted in K scenarios
Clogging Factor	Clogging parameter (clogging ignored)	0	-
Drain Layer			
Flow Coefficient	Determines drain flow rate as a function of hydraulic head (C)	0.6	County (2008)
Flow Exponent	Determines drain flow rate as a function of hydraulic head (n)	0.5	County (2008)
Offset	Drain height above bottom of storage layer (cm)	15	Miller (1978)

Table 3: Bioretention design configurations used in New Build and Retrofit scenarios.

New Build Scenario Design Configurations:

Ponding: All BASE parameters held constant except Berm Height

Configuration	Berm Height (cm)
P1	15
P2	30
P3	61

Media Depth: All BASE parameters held constant except Thickness (soil layer)

Configuration	Thickness (cm)
DEP1	61
DEP2	91
DEP3	122

Media Conductivity: All BASE parameters held constant except Conductivity

Configuration	Conductivity (mm/hr)
CON1	51
CON2	76
CON3	102

Surface Area: All BASE parameters held constant except Area

Configuration	Area (percent of drainage area)
A1	5%
A2	10%
A3	15%

Composite Configurations: All BASE parameters held constant except the following:

Configuration	Berm Height (cm)	Thickness (cm)	Conductivity (mm/hr)	Area (% Catchment)
LOW	15	61	51	5%
MID	30	91	76	10%
HIGH	46	122	102	15%

Retrofit Scenario Design Configurations:

Retrofit Configurations: All BASE parameters held constant except the following:

Configuration	Berm Height (cm)	Thickness (cm)
R1	15	91
R2	30	76
R3	46	61
R4	61	46

In total, 15 designs were analyzed under the New Build scenario. Parameters were individually adjusted to assess their impact on future performance and illustrate where priority should be placed when considering additional investments in bioretention design. Composite configurations containing a combination of these designs were also tested. Table 3 also details the four configurations tested in the Retrofit scenario (R1-R4). The surface storage depth in scenario R4 (approximately 61 cm) is double the maximum ponding depth recommended in local regulations (TDEC, 2014). Additionally, the media depth is reduced to 46 cm in this design. Beyond performance implications, safety hazards, prolonged surface ponding, and impacts to plant health could be expected if this design were implemented. However, this was considered to illustrate the lengths that may be required to retrofit an existing system to maintain performance under future conditions.

The BASE design configuration (Table 2) was modeled with observed rainfall data (2010-2014) to compare the New Build and Retrofit results against historic performance. Bioretention configurations were modeled using three underlying soil types (i.e., K1, K2, and K3) to assess the impact of site-specific conditions on bioretention hydrology under climate change. The underlying soils included clay (K_{sat} = 1.27 mm hr^{-1}, K1), clay loam (K_{sat} = 12.7 mm hr^{-1}, K2), and sandy loam (K_{sat} = 25.4 mm hr^{-1}, K3).

2.5 Future climate data

Climate change projections were downloaded from the North American Coordinated Regional Downscaling Experiment (NA-CORDEX) Program (Mearns et al., 2017; Unidata Science Gateway, 2020). Projections are derived from RCMs which use boundary conditions created from GCMs in the Coupled Model Intercomparison Project 5 (CMIP5) database (Mearns et al., 2017). Only projections containing hourly rainfall data were used to better represent the hydrologic response times of urban areas (Zahmatkesh et al., 2015). As a result, ten dynamically downscaled projections of hourly rainfall data over a five-year period were used in this study (Table 4).

Table 4: Description of hourly climate models used in this study.

Model No.	GCM	RCM	RCP	Spatial Resolution
1	CanESM2	CanRCM4	4.5	50 km
2	CanESM2	CanRCM4	8.5	50 km
3	GFDL-ESM2M	WRF	8.5	25 km
4	GFDL-ESM2M	WRF	8.5	50 km
5	HadGEM2-ES	WRF	8.5	25 km
6	HadGEM2-ES	WRF	8.5	50 km
7	MPI-ESM-LR	RegCM4	8.5	25 km
8	MPI-ESM-LR	RegCM4	8.5	50 km
9	MPI-ESM-LR	WRF	8.5	25 km
10	MPI-ESM-LR	WRF	8.5	50 km

The majority of the RCPs available from the hourly NA-CORDEX archive used the RCP8.5 emissions scenario, representing continued population growth, anthropogenic emissions, and energy consumption (IPCC, 2014). Though technological advances, emissions reductions, and human adaptations could mitigate future climate changes and impacts on bioretention hydrology, this was embraced to illustrate the magnitude of action that required to impact future bioretention performance. Further, the intent of the study was not to compare differences in bioretention performance between possible RCPs.

2.6 Bias correction

Climate models regularly overestimate the frequency of low intensity rainfall while underestimating occurrences of intense rain, referred to as the “drizzle problem” (Sun and Solomon, 2005; Stephens et al., 2010). Because RCM outputs represent averages of larger grids (i.e., 25 km or 50 km grids), the data must be adjusted to fit the scale of observed values at a location of interest (Cook et al., 2019; Cook et al., 2020). Thus, bias correction (BC) procedures should be implemented before RCM outputs are used in hydrologic models (Rosenberg et al., 2010).

Kernel density distribution mapping (KDDM), a novel non-parametric technique developed by McGinnis et al. (2015), was used to correct climate model bias. Distribution mapping techniques such as KDDM adjust individual values within climate model output to match their statistical distribution with that of an observed data set (McGinnis et al., 2015). The KDDM method fits a transfer function between the empirical cumulative distribution functions (CDFs) of observed rainfall and climate model output for a historical time period to adjust future climate data to the scale of the observed data (McGinnis et al., 2015; Cook et al., 2019; Cook et al., 2020). Based on available rainfall data for Knoxville, 1997-2011 was chosen for the historical period, and 2035-2049 for the future period for bias correction.

The KDDM bias correction procedure was performed on both hourly rainfall and temperature (daily maximum and minimum) datasets that were used in the hydrologic models using the R package "climod" (McGinnis, 2018). Bias correction of temperature projections was performed on a monthly basis to account for natural, seasonal variations (which can be much larger than model bias) (McGinnis et al., 2015). The statistical similarities of the observed data and bias corrected climate model output for the historical period were confirmed using the Wilcoxon rank sum test, which was concluded after observing that the null hypothesis could be accepted for all ten models following bias correction (R Core Team, 2019). Subsets of bias corrected temperature and rainfall data for the period of interest (2040-2044) were then inputted to SWMM models. More information on the KDDM bias correction procedure can be found in McGinnis et al. (2015) and the climod documentation (McGinnis, 2018).

2.7 Performance metrics

Three components of the annual water balance (surface overflow, infiltration, and drain outflow) were used to compare future bioretention performance in the New Build and Retrofit scenarios against past performance. The proportion of climate projections leading to improved future performance relative to historic levels (by both annual volumes diverted to each pathway as well as their percentage of the overall water balance) was determined and compared across design configurations to characterize their impact on performance (Table 3). The procedure followed in this analysis is shown in Figure 1.

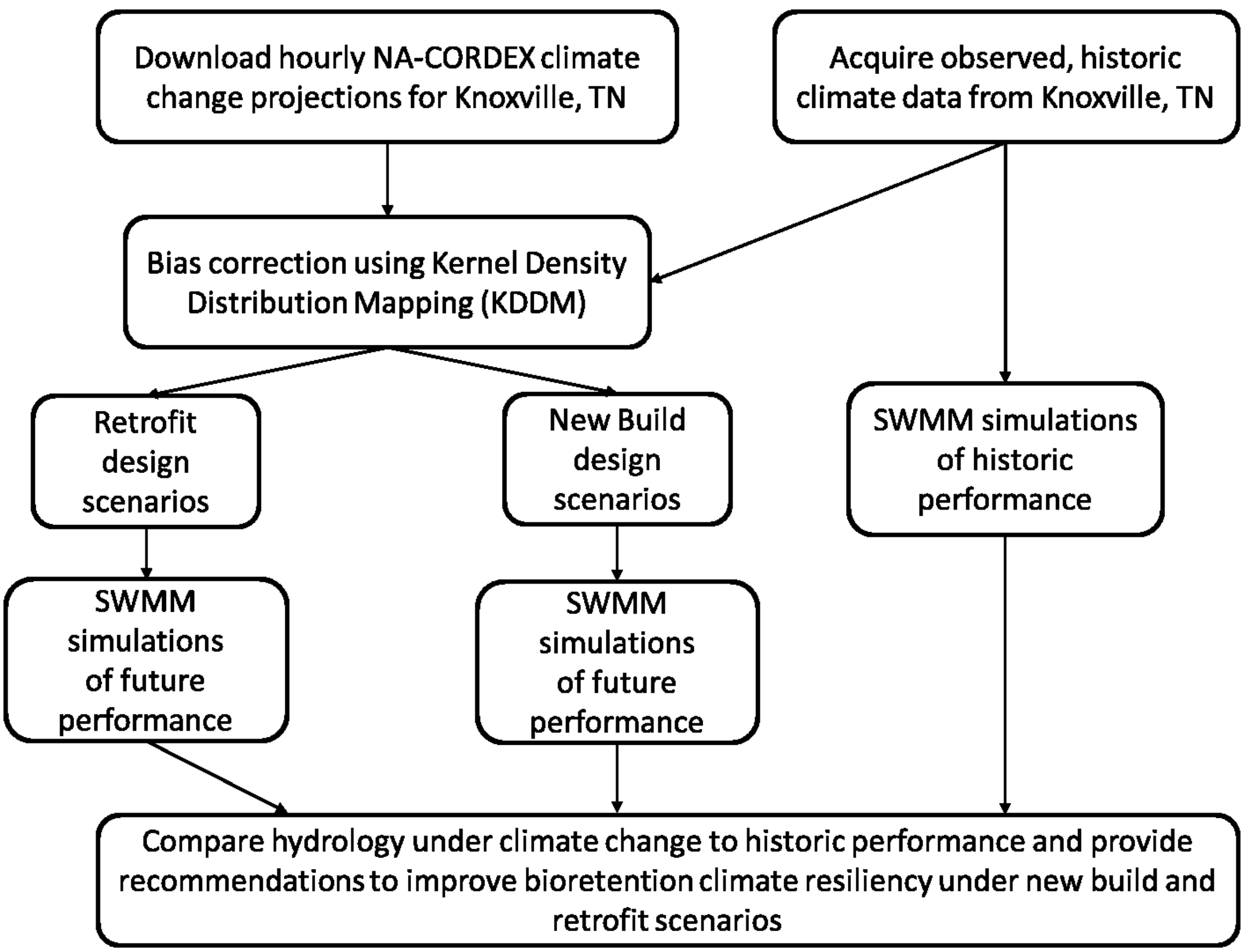

Figure 1: Flowchart of work process.

3.0 Results and Discussion

3.1 Climate change projections

Summary statistics for the bias corrected climate projections (2040-2044) and observed climate data (2010-2014) are shown in Table 5. Compared to the observed data from 2010-2014, model projections averaged more annual rainfall (a mean of 1731 mm across all ten projections) which was delivered in a higher number of rain events (annual mean of 98 events, data not shown) and separated by shorter dry periods (mean antecedent dry period (ADP) of 3.8 days) compared to historic observations (mean annual rainfall of 1310 mm delivered in 84 events separated by a mean ADP of 4.3 days). Median storm sizes in future projections were generally less than historic conditions, while on average, GCMs projected the size of the 90th percentile rain event will be approximately 29% larger in the future period (44 mm) compared to historic conditions (34 mm). This finding agrees with previous studies which report the impact of climate change on larger storms with less-frequent return periods (e.g., Olsson et al., 2009; Kim and Choi, 2011; Wang et al., 2019a).

Other rainfall parameters varied across the GCMs. Nine of the ten models predicted more rainfall and shorter dry periods than historic observations. Similarly, peak storm intensities varied across the projections compared to historic conditions. Some models (i.e., models 4, 5, 8, and 10) contained elevated 90th percentile peak storm intensities, in line with research suggesting that future rain events will become more frequent and intense under climate change (USGCRP, 2018). However, other projections predicted lower peak rainfall intensities. Zhang et al. (2019) found similar variability in assessing climate change projections for Melbourne, Australia, as the amount of rainfall, duration of dry periods, and maximum and average intensities varied across the eight GCMs used in their study.

Taken together, the GCM projections illustrate the importance of addressing the uncertainty of future climate changes. For example, were future conditions similar to those predicted in model 9, the deviations from historic conditions (i.e., slightly more annual rainfall with similar inter-event dry periods and peak rainfall intensities) may allow existing GI practices to manage future runoff without the need for modifications. However, this is unlikely if future conditions were to resemble those predicted by model 5; a 226% increase in annual rainfall and 172% increase in 90th percentile peak rainfall intensity would likely exceed the capacity of bioretention cells designed and constructed based on historic conditions. Such conditions may also threaten the health of microbes and plants through inundation during larger rain events, potentially limiting the treatment benefits they provide (Manka et al., 2016; Zhang et al., 2019). While some projections contain larger deviations than others, even small changes in climate may be exacerbated in highly responsive urban catchments, often characterized by a high percentage of impervious cover (Wang et al., 2019b). As such, the differences in model projections were recognized to reflect the inherent uncertainty in predicting future climate.

Table 5: Summary statistics for precipitation and temperature for climate change projections (2040-2044) and observed data (2010-2014).

	Rainfall				Dry Period				Average Daily Temperature			
Model	Mean Annual Rain (mm/yr)	90th Percentile Peak Event Intensity (mm/hr)	Median Event Depth (mm)	Avg. Annual Rain Days	Mean (days)	Median (days)	St. Dev. (days)	90th Percentile Dry Period (days)	Mean (°C)	Median (°C)	Max (°C)	Min (°C)
1	1611	9.7	4.7	164	3.1	2.0	2.9	6.9	15.2	16.2	32.9	-8.8
2	1465	8.5	4.8	155	3.2	1.7	3.2	7.3	15.3	16.5	31.1	-7.6
3	1626	11.6	5.1	185	3.4	2.0	3.7	7.8	15.5	16.7	29.7	-9.1
4	1749	13.7	7.6	136	4.3	3.0	4.0	9.6	15.5	16.7	29.3	-8.8
5	2958	21.9	9.4	152	3.4	2.3	3.0	7.5	15.0	15.7	32.1	-14.1
6	1745	12.7	6.3	136	3.9	2.7	3.7	9.0	15.0	15.9	33.5	-14.3
7	1310	11.9	6.8	136	4.3	3.3	3.4	8.6	15.5	16.5	30.9	-12.5
8	1780	14.9	8.5	134	4.3	3.2	3.9	8.7	15.3	16.0	31.1	-8.4
9	1484	12.7	8.4	140	4.1	3.0	3.4	8.8	15.1	16.1	30.6	-16.1
10	1588	13.4	8.9	132	4.3	3.2	4.0	9.0	15.1	16.1	31.4	-16.2
Observed	1310	12.7	9.4	139	4.3	3.8	2.9	8.6	15.4	16.5	32.3	-11.7

3.2 New Build scenario

Simulation results for the New Build design scenarios (Table 2) are summarized in Figures 2 and 3. Results show that current designs may be sufficient under some future climate scenarios that represent lower deviations from current climate but are overwhelmed in others, and that site-specific considerations should be made when modifying bioretention designs for the future (Moore et al., 2016; Zhang et al., 2109). As expected, the underlying soil conditions impacted annual infiltration and drain outflow volumes. Increased annual infiltration volumes were observed in the well-drained soils in the K3 scenario compared with poorly drained soils (K1) (Figure 2). Further, a greater number of climate projections met or exceeded historic infiltration volumes in the K2 and K3 scenarios compared with K1. This suggests that more conservative design amendments (e.g., increased temporary ponded storage) could have greater impacts at sites with moderate to well-drained *in situ* soils compared to poorly-drained soils, where more significant modifications (e.g., increased surface areas or implementing several modifications simultaneously such as those in the MID and HIGH scenarios) are needed to meet historic infiltration volumes. Conversely, drain outflow volumes increased as soil drainage decreased; models showed that water readily percolated into the rapidly draining soils in scenarios K2 and K3, while water exiting the practice via the underdrain occurred more frequently in the poorly drained soils in K1.

Unlike infiltration and drain outflow, underlying soil properties had little effect on annual surface overflow volumes; modeled surface overflow for many design configurations across all K scenarios exceeded historic surface levels (Figure 2). Other studies have reported increased surface overflow from bioretention cells under future climate conditions (e.g., Olsson et al., 2009; Hathaway et al., 2014), as increased depths and variable intensities of future rainfall can overwhelm bioretention infiltration rates and limited volumes for temporary ponded storage. Because this represents runoff that bypassed any treatment or hydrologic mitigation provided by the practice, it may be an indication that more significant modifications are needed regardless of site conditions to reduce the impacts of future runoff, as most models using the MID or HIGH design configurations reduced surface overflow volumes beyond historic levels.

Trends in future performance were largely consistent across the various soil types with respect to water balance composition (Figure 3). In general, while the magnitude of each water balance component shifted between K scenarios, simulations for most configurations resulted in proportionally lower infiltration and higher surface overflow compared to historic conditions, while drain outflow was mixed. As with surface overflow volumes, the bioretention water balance may be heavily influenced by shifting rainfall patterns (e.g., more annual rainfall, increased magnitudes of larger events, etc.). While many design modifications improved infiltration volumes in K2 and K3 scenarios, the trends in Figure 3 suggest that projected future rainfall (Table 5) will limit the ability of bioretention cells to maintain a water balance similar to historic conditions in all but the most intensive deviations from current design practices, as consistent improvements were largely limited to A3, MID, and HIGH regardless of underlying soil conditions.

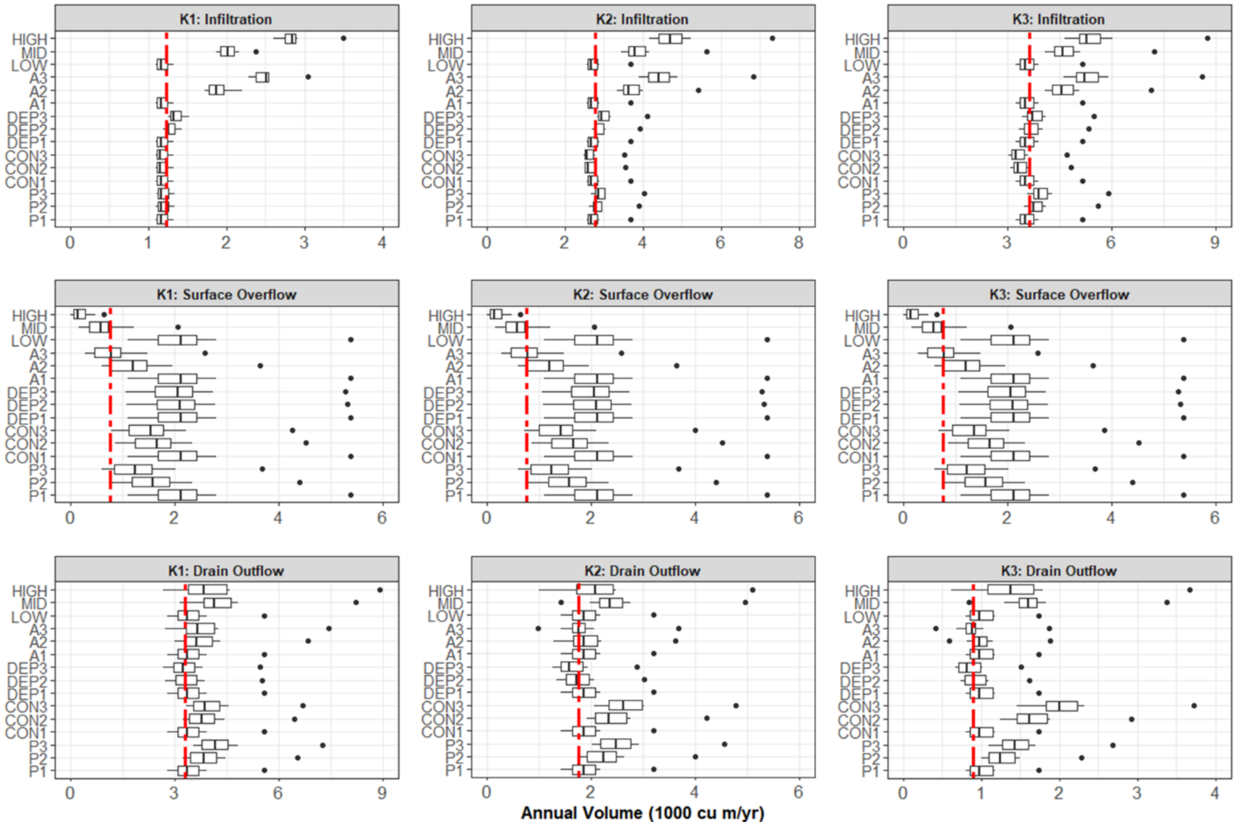

Figure 2: Box plots summarizing future (2040-2044) bioretention performance with various design modifications under climate uncertainty. Plots show annual volumes directed to infiltration, surface outflow, or drain outflow under three underlying soil conditions (K1: poorly-drained, K2: moderately-drained, K3: well-drained). Annual volumes derived from model results of historic bioretention performance using current design standards and observed rainfall records from 2010-2014 corresponding to each pathway and scenario are indicated by dashed vertical red lines in each plot.

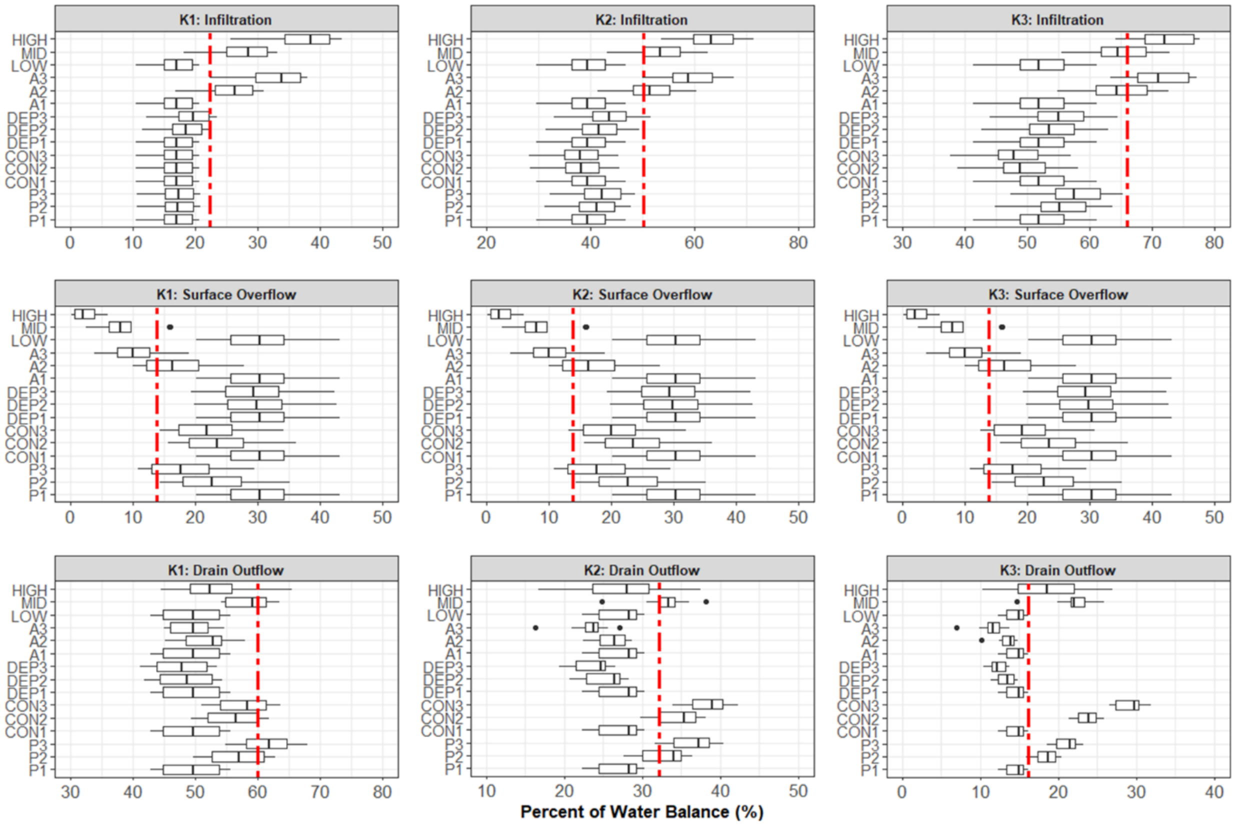

Figure 3: Box plots summarizing future (2040-2044) bioretention performance with various design modifications under climate uncertainty. Plots show the percentage of the overall water balance comprised of infiltration, surface outflow, or drain outflow under three underlying soil conditions (K1: poorly-drained, K2: moderately-drained, K3: well-drained). The portions of the water balance based on model results of historic bioretention performance using current design standards and observed rainfall records from 2010-2014 corresponding to each pathway and scenario are indicated by dashed vertical red lines in each plot.

The percentiles corresponding to historic performance, as well as the performance returns (defined as increases in the percentage of future scenarios meeting or surpassing historic levels) for each design modification are shown in Table 6. Depending on management objectives and site conditions, these results illustrate where priority should be placed to incorporate resiliency to future climate conditions. For example, if the primary management objective was to maximize runoff reduction by promoting infiltration from bioretention cells in areas with poor to moderately-drained soils, increasing the depth of the media layer within the practice provides the greatest returns relative to other, more conservative design modifications (e.g., increasing saturated conductivity of media). However, increasing ponding depths provides the greatest improvements to infiltration performance for sites with well-drained soils (K3).

Table 6: Comparison of historic bioretention performance (2010-2014) compared to model results of modified designs under future climate scenarios (2040-2044). Values represent the percentile corresponding to historic performance relative to the range of future model results. Percentiles based on annual volumes are listed next to those based on water balance composition, which are reported in parentheses. Performance returns for each design component are shown as the absolute value of the difference between the minimum and maximum design in each configuration group.

	K1			K2			K3		
	Infiltration	Surface	Drainage	Infiltration	Surface	Drainage	Infiltration	Surface	Drainage
P1	72.5 (100)	0 (0)	39.2 (100)	68.3 (100)	0 (0)	35.4 (100)	67.0 (100)	0 (0)	28.5 (100)
P2	71.5 (100)	0 (0)	7.1 (68.5)	47.2 (100)	0 (0)	0 (33.8)	37.9 (100)	0 (0)	0 (9.3)
P3	70.8 (100)	22.3 (26.8)	0 (40.8)	18.0 (100)	22.3 (26.8)	0 (6.0)	12.9 (100)	22.3 (26.8)	0 (0)
|P3-P1|	1.7 (0)	22.3 (26.8)	39.2 (59.2)	50.3 (0)	22.3 (26.8)	35.4 (94.0)	54.1 (0)	22.3 (26.8)	28.5 (100)
CON1	72.5 (100)	0 (0)	39.2 (100)	68.3 (100)	0 (0)	35.4 (100)	67.0 (100)	0 (0)	28.5 (100)
CON2	73.3 (100)	0 (0)	10.8 (74.6)	77.4 (100)	0 (0)	0 (24.3)	83.3 (100)	0 (0)	0 (0)
CON3	73.3 (100)	0 (0)	0 (63.0)	84.6 (100)	2.9 (10.5)	0 (0)	89.2 (100)	5.8 (23.3)	0 (0)
|CON3-CON1|	0.8 (0)	0 (0)	39.2 (59.2)	16.3 (0)	2.9 (10.5)	0 (0)	22.2 (0)	5.8 (23.3)	28.5 (100)
DEP1	72.5 (100)	0 (0)	39.2 (100)	68.3 (100)	0 (0)	35.4 (100)	67.0 (100)	0 (0)	28.5 (100)
DEP2	45.3 (100)	0 (0)	53.0 (100)	36.3 (100)	0 (0)	57.5 (100)	51.5 (100)	0 (0)	49.6 (100)
DEP3	0 (79.4)	0 (0)	57.9 (100)	0 (93.0)	0 (0)	65.6 (100)	39.5 (100)	0 (0)	64.2 (100)
|DEP3-DEP1|	72.5 (20.6)	0 (0)	18.7 (0)	68.3 (7.0)	0 (0)	30.2 (0)	27.5 (0)	0 (0)	35.7 (100)
A1	72.5 (100)	0 (0)	39.2 (100)	68.3 (100)	0 (0)	35.4 (100)	67.0 (100)	0 (0)	28.5 (100)
A2	0 (10.6)	24.2 (28.6)	26.2 (100)	0 (36.3)	24.2 (28.6)	38.5 (100)	0 (68.7)	24.2 (28.6)	20.4 (100)
A3	0 (0)	48.6 (79.8)	21.6 (100)	0 (0.4)	48.6 (79.8)	51.7 (100)	0 (18.4)	48.6 (79.8)	60.7 (100)
|A3-A1|	72.5 (100)	48.6 (79.8)	17.6 (0)	68.3 (100)	48.6 (79.8)	16.3 (0)	67.0 (81.6)	48.6 (79.8)	32.2 (0)
LOW	72.5 (100)	0 (0)	39.2 (100)	68.3 (100)	0 (0)	35.4 (100)	67.0 (100)	0 (0)	28.5 (100)
MID	0 (7.2)	78.3 (85.4)	5.8 (59.0)	0 (24.6)	78.3 (85.4)	6.9 (24.6)	0 (68.4)	78.3 (85.4)	1.3 (3.2)
HIGH	0 (0)	100 (100)	18.4 (93.1)	0 (0)	100 (100)	31.0 (90.1)	0 (15.0)	100 (100)	9.0 (35.0)
|HIGH-LOW|	72.5 (100)	100 (100)	20.8 (6.9)	68.3 (100)	100 (100)	4.4 (9.9)	67.0 (85.0)	100 (100)	19.5 (65.0)

Other modifications should be considered if objectives are centered on reducing untreated, unmitigated surface overflows. Increasing ponding depths should be prioritized over deepening media layers or increasing media saturated conductivity for sites in all soil types, allowing more water to be stored within the bioretention surface layer before percolating into the media. Increasing media conductivities provided modest improvements in surface overflow for sites with moderate- to well-drained soils; however, this modification may influence hydraulic retention times and correspondingly impact the pollutant removal that could occur within the cell. Finally, priority should be placed on deepening media layers if management objectives are focused on reducing drainage outflows and retaining runoff on-site, as designs with increased media thickness (i.e., DEP3) resulted in the highest number of simulations falling below historic drainage levels in all K scenarios. Unlike increasing saturated conductivities, deepening media profiles may provide greater opportunities for pollutant removal within the system, as well as potentially improved plant health due to increased soil volumes, which foster root exploration and water storage during inter-event dry periods (Read et al., 2008; Hatt et al., 2009; Le Coustumer et al., 2012).

Increasing bioretention surface area relative to the catchment area had the largest effect on overall performance in every K scenario. Increasing bioretention surface area to 15% of the contributing catchment resulted in all of climate scenarios surpassing historic annual infiltration volumes. The largest impact of surface area modification occurred in the K1 scenario, as 100% of future simulations surpassed historic annual volumes and proportional amounts of infiltration using the A3 design compared to 27.5% and 0% in the A1 design, respectively. Simulations of the K2 scenario followed these trends, surpassing performance improvements observed in the K3 scenario with respect to infiltration. This suggests that expanding surface area in new bioretention installations may become increasingly important to incorporate resiliency to future climate change as the infiltration capacities of underlying soils decline.

Increasing bioretention surface area also led to the largest improvements with respect to minimizing surface overflow and drainage outflows. As surface overflows were mostly influenced by rainfall parameters, surface area increases led to similar reductions in overflow regardless of underlying soils. Practices designed with a surface area equal to 15% of the contributing catchment surpassed historic levels with respect to annual volumes and proportion of the water balance in 48.6% and 79.8% of climate simulations, respectively, compared with 0% of simulations meeting historic levels when surface areas were equal to 5% of the catchment. Interestingly, drainage outflows were minimized in the K3 scenario using the A2 configuration. This may be attributable to lower surface overflows in these simulations, which resulted in more runoff percolating through the practice that contributed to both infiltration and drainage outflow. As increasing surface area yielded the largest impact to future performance, the composite configurations (LOW, MID, HIGH) followed similar trends observed in the A1, A2, and A3 simulations. However, further improvements were evident in these trials. Reduced effects were once again observed as drainage of underlying soils increased, suggesting that intensive design modifications should be considered in areas with poorly draining soils where elevated risks posed by future climate change are anticipated.

These conclusions support findings from other studies of the effects of climate uncertainty on LID performance. Studies such as Eckart et al. (2018), Zhang et al. (2019), and Wang et al. (2019a and 2019b) concluded that larger bioretention surface areas would be needed to ensure their performance under future climate conditions. Similar to observations by Wang et al. (2019a), incremental runoff reduction decreased as the bioretention surface area increased, as the largest improvements with respect to infiltration occurred between the A1 and A2 (and LOW to MID) configurations. Likewise, the largest improvements to surface overflow performance occurred between the LOW and MID configurations. Because these designs correspond to increased investment in the practice compared to modifying the other parameters, management objectives should be considered prior to their implementation.

3.3 Retrofit scenario

Results of the Retrofit modifications (Table 2) under future climate conditions are summarized in Figures 4 and 5, while the percentiles corresponding to historic performance and returns for each retrofit measure are shown in Table 7. As with the ponding configurations in the New Build scenario, increasing ponding depths (by subsequently decreasing the media layer thickness) consistently improved surface overflow performance across all underlying soil types. However, historic performance was exceeded for the majority of trials in even the highest retrofit measures, with 71.1 % and 67.4% of simulations exceeding annual volumes and the proportion of the water balance corresponding to surface overflows, respectively. Further, given that storage depths in the R4 scenario are substantially higher than permitted depths in many jurisdictions (e.g., NCDEQ, 2009, TDEC, 2014, MPCA, 2016), the increased risks to public health and safety may make these designs impractical.

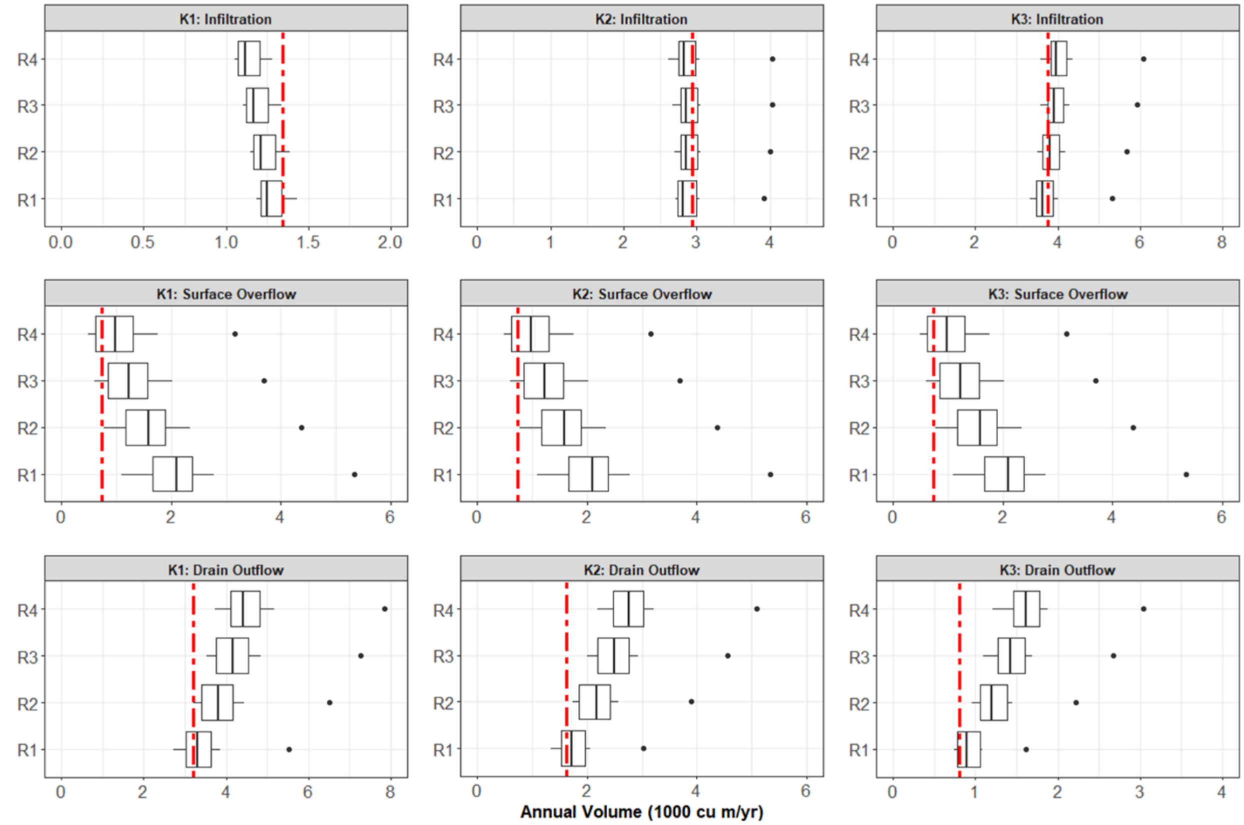

Figure 4: Box plots summarizing future (2040-2044) bioretention performance with various retroactive modifications implemented to add resiliency under climate uncertainty. Plots show annual volumes directed to infiltration, surface outflow, or drain outflow under three underlying soil conditions (K1: poorly-drained, K2: moderately-drained, K3: well-drained). Annual volumes derived from model results of historic bioretention performance using current design standards and observed rainfall records from 2010-2014 corresponding to each pathway and scenario are indicated by dashed vertical red lines in each plot.

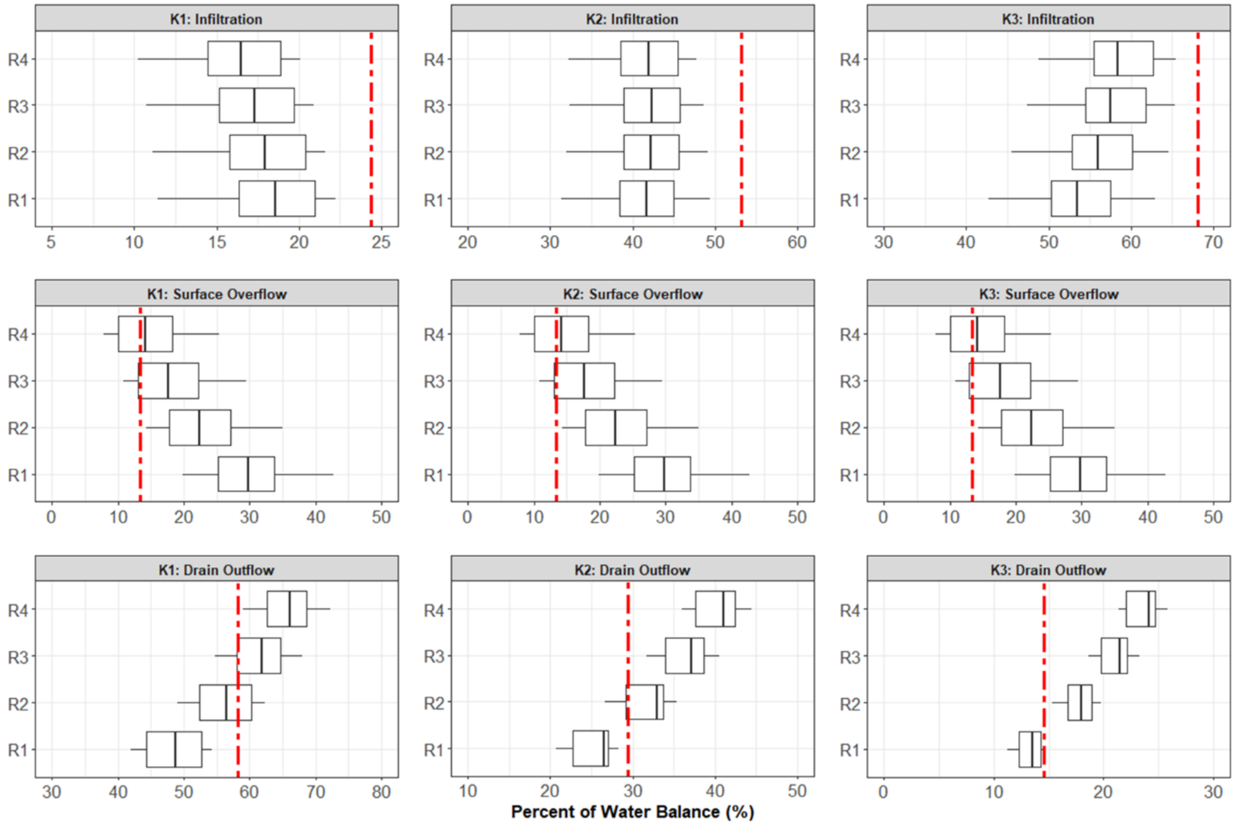

Figure 5: Box plots summarizing future (2040-2044) bioretention performance with various retroactive modifications implemented to add resiliency under climate uncertainty. Plots show the percentage of the overall water balance that is comprised of infiltration, surface outflow, or drain outflow under three underlying soil conditions (K1: poorly-drained, K2: moderately-drained, K3: well-drained). The portions of the water balance based on model results of historic bioretention performance using current design standards and observed rainfall records from 2010-2014 corresponding to each pathway and scenario are indicated by dashed vertical red lines in each plot.

Table 7: Comparison of historic bioretention performance (2010-2014) compared to model results using retroactive modifications future climate scenarios (2040-2044). Values represent the percentile of the range of future model results corresponding to historic performance for various hydrologic pathways, underlying soil conditions, and retrofit measures. Percentiles based on annual volumes are listed next to those based on water balance composition, which are reported in parentheses. Performance returns for each scenario are shown as the absolute value of the difference between R4 and R1.

K Scenario	Configuration	Infiltration	Surface	Drainage
K1	R1	75.7 (100)	0 (0)	36.8 (100)
	R2	82.8 (100)	0 (0)	0.7 (61.3)
	R3	100 (100)	16.0 (25.8)	0 (33.8)
	R4	100 (100)	28.9 (32.6)	0 (0)
	|R4-R1|	24.3 (0)	28.9 (32.6)	36.8 (100)
K2	R1	68.4 (100)	0 (0)	32.4 (100)
	R2	67.3 (100)	0 (0)	0 (26.0)
	R3	69.4 (100)	16.0 (25.8)	0 (0)
	R4	71.1 (100)	28.9 (32.6)	0 (0)
	|R4-R1|	2.7 (100)	28.9 (32.6)	32.4 (100)
K3	R1	66.3 (100)	0 (0)	27.6 (82.0)
	R2	44.0 (100)	0 (0)	0 (0)
	R3	26.4 (100)	16.0 (25.8)	0 (0)
	R4	16.9 (100)	28.9 (32.6)	0 (0)
	|R4-R1|	49.4 (0)	28.9 (32.6)	27.6 (82.0)

Hathaway et al. (2014) determined that storage depths would need to be increased by 9-31 cm (while holding other design parameters constant) to restrict annual overflow from bioretention cells to a baseline scenario under future climate conditions in North Carolina, USA. In a similar study demonstrating the geographic differences of climate impacts on bioretention hydrology, Winston (2016) found that increasing ponding depths by up to 51% (corresponding to an additional 5-17 cm) was necessary to maintain historic surface overflows from a bioretention cell in northeast Ohio, USA. Simulation results from the Retrofit scenario indicate that even more storage may be necessary to reduce future surface overflow. This suggests that other retrofit measures may need to be considered to improve surface overflow performance. For example, as suggested by the New Build scenario results (Table 6), replacing existing media with a more rapidly draining mixture in combination with modifying ponding depths may provide additional improvements in bioretention performance in sites with well-drained soils.

While marginally increased volumes were directed toward infiltration in well-drained soils, the portion of the water balance representing infiltration in historic conditions was not achieved in any of the Retrofit configurations. Performance based on annual infiltration volumes slightly declined in the K1 scenario as retrofit measures increased from R1 to R4 yet remained relatively similar across K2 trials. The hydrologic impact of the retrofit measures in the future period was most apparent with respect to drainage outflows. Across all K scenarios, the proportion of simulations with elevated levels of drainage outflows increased with increasing retrofit measures (i.e., between R1 and R4). However, while drainage outflows represent runoff receiving treatment from the practice, the decreased bioretention media thickness in the Retrofit scenario (especially in the R3 and R4 configurations) may limit the pollutant removal capabilities of the cell due to decreased retention times and soil volumes available for plant roots, resulting in a diminished quality of drainage. Based on these results and the limited reduction to surface overflows and the risks to public health and safety associated with these designs, the proposed retrofit measures may not provide a feasible path to incorporating resiliency to climate change in existing bioretention facilities.

4.0 Conclusions and Recommendations

Climate change poses risks to GI such as bioretention cells to effectively manage urban stormwater runoff in the coming decades. Simulations using EPA SWMM 5.1 and bias corrected climate model output were analyzed using a probabilistic approach to evaluate the efficacy of bioretention design modifications and retrofit measures to add resiliency to bioretention cells in the face of future climate uncertainty. Results indicated that the greatest return on historic performance occurred when increased surface areas (relative to the contributing catchment) are used in design, especially in sites with moderate to poorly drained *in situ* soils. However, while retrofits to existing bioretention cells reduced untreated surface overflows in future simulations, the marginal performance returns, risks to public health and safety, and potentially diminished treatment capacities of these designs may not represent a realistic option to incorporate climate resiliency into existing practices.

Findings also demonstrate the attention that must be directed to management objectives, risk tolerance, and local site conditions when assessing options to ensure bioretention effectiveness in future climate conditions. Depending on underlying soil characteristics, results suggest that design modifications had various impacts to bioretention hydrology, which should be considered with respect to management objectives such as minimizing surface overflows or maximizing runoff reduction via infiltration. In several instances, current design standards met or exceeded historic performance levels for a subset of future climate projections. In locations where stormwater engineers or officials are willing to accept the likelihood that most climate projections will lead to future performance declines, increased investment in bioretention design may not be necessary. However, modifying bioretention designs, such as the use of larger practices, may be critical in more risk averse communities to ensure their effective operation in the future.

Future studies should incorporate this methodology with a larger set of climate models, emissions scenarios, and study locations to more broadly understand the impacts of climate change on bioretention performance. Studies should add to the combination of design factors, consider the effects of clogging and media degradation over time (e.g., decreases in media porosity and field capacity) on the viability of retrofit measures, and consider the economic impacts of modified designs to identify optimal methods to enhance bioretention resiliency to future climate uncertainty with respect to infrastructure costs. Research should be conducted to investigate the impacts of climate change on the pollutant removal performance of bioretention cells. Finally, this assessment is predicated on a desire to maintain historical function into the future, but different interventions affect different hydrologic pathways. There is a need for broader discussion in the urban watershed management community to clearly define resiliency in their context.

Acknowledgements

This material is based upon work supported by the National Science Foundation under Grant No. 1634975. The authors would like to thank Dr. Seth McGinnis and Dr. Lauren Cook for their assistance with the bias correction procedure and Dr. Sean Arms for his assistance in acquiring the climate projections used in this research.

References

Anandhi, A., A. Frei, D. C. Pierson, E. M. Schneiderman, M. S. Zion, D. Lounsbury, and A. H. Matonse (2011). "Examination of change factor methodologies for climate change impact assessment". Water Resources Research, 47, W03501.

Arnold, C. L., and C. J. Gibbons (1996). "Impervious surface coverage: the emergence of a key environmental indicator". Journal of the American Planning Association, 62(2), 243-258.

Barah, M., A. Khojandi, X. Li, J. Hathaway, and O. Omitaomu (2020). "Optimizing green infrastructure placement under precipitation uncertainty". Accepted, Omega, DOI: https://doi.org/10.1016/j.omega.2020.102196.

Berggren, K., M. Olofsson, M. Viklander, G. Svensson, and A. Gustafsson (2012). "Hydraulic impacts on urban drainage systems due to changes in rainfall caused by climatic change". Journal of Hydrologic Engineering, 17(1), 92-98.

Berliner, L. M. (2003). "Uncertainty and climate change". Statistical Science, 18(4), 430-435.

Booth, D. R., and C. R. Jackson (1997). "Urbanization of aquatic systems: degradation thresholds, stormwater detection, and the limits of mitigation". Journal of the American Water Resources Association, 33(5), 1077-1090.

Brakensiek, D., R. Engleman, and W. Rawls (1981). "Variation within texture classes of soil water parameters". Transactions of the ASAE, 24(3), 0335-0339.

Brown, R. A., and W. F. Hunt (2011). "Underdrain configuration to enhance bioretention exfiltration to reduce pollutant loads". Journal of Environmental Engineering, 137(11), 1082-1091.

Committee, M.S.S. (2005). The Minnesota Stormwater Manual. Developed by Emmons and Olivier Resources for the Stormwater Steering Committee. Minnesota Pollution Control Agency, St. Paul, MN, Paul, MN.

Cook, L., C. Samaras, and J. M. VanBriesen (2019). "Using rainfall measures to evaluate hydrologic performance of GI under climate change". Sustainable and Resilient Infrastructure. DOI: 10.1080/23789689.2019.1681819.

Cook, L., S. McGinnis, and C. Samaras (2020). "The effect of modeling choices on updating intensity duration frequency curves and stormwater infrastructure designs for climate change". Accepted, Climatic Change, DOI: 10.1007/s10584-019-02649-6.

County, K. (2008). Knox County Tennessee Stormwater Management Manual. Knox County, Knoxville, TN.

Davis, A. P., W. F. Hunt, R. G. Traver, and M. Car (2009). “Bioretention technology: overview of current practice and future needs”. Journal of Environmental Engineering, 135(3), 109-117.

DeBusk, K. M. and T. M. Wynn (2011). “Storm-water bioretention for runoff quality and quantity mitigation”. Journal of Environmental Engineering, 137(9), 800-808.
Denault, C., R. G. Millar, and B. J. Lence (2006). “Assessment of possible impacts of climate change in an urban catchment”. Journal of the American Water Resources Association, 42(3), 685-697.

Eckart, K., Z. McPhee, and T. Bolisetti (2018). “Multiobjective optimization of low impact development stormwater controls”. Journal of Hydrology, 562, 564-576.

Hargreaves, G. H., and Z. A. Samani (1985). “Reference crop evapotranspiration from temperature”. Applied Engineering in Agriculture, 1(2), 96-99.

Hathaway, J. M., R. A. Brown, J. S. Fu, and W. F. Hunt (2014). “Bioretention function under climate change scenarios in North Carolina, USA”. Journal of Hydrology, 519, 503-511.

Hatt, B. E., T. D. Fletcher, and A. Deletic (2009). “Hydrologic and pollutant removal performance of stormwater biofiltration systems at the field scale”. Journal of Hydrology, 365(3–4), 310–321.

Hollis, G. E. (1975). “The effect of urbanization on floods of different recurrence interval”. Water Resources Research, 11(3), 413-435.

IPCC (2014). Climate Change 2014: Synthesis Report. Contribution of Working Groups I, II and III to the Fifth Assessment Report of the Intergovernmental Panel on Climate Change [Core Writing Team, R.K. Pachauri and L.A. Meyer (eds.)]. IPCC, Geneva, Switzerland, 151 pp.

Kim, E. S., and H. I. Choi (2011). "Assessment of vulnerability to extreme flash floods in design storms." International Journal of Environmental Research and Public Health, 8(7), 2907-2922.

Klein, R. D. (1979). “Urbanization and stream quality impairment”. Journal of the American Water Resources Association, 15(4), 948-963. Journal of Hydrologic Engineering, 14(4), 407-415.

Le Coustumer, S., T. D. Fletcher, A. Deletic, S. Barraud, and P. Poelsma (2012). “The influence of design parameters on clogging of biofilters: a large-scale column study”. Water Research, 46, 6743-6752.

Leopold, L. (1968). “Hydrology for Urban Land Planning: A Guidebook on the Hydrologic Effects of Urban Land Use”. Geological Survey Circular, 554, United States Department of the Interior, Washington, D.C.

McGinnis, S., D. Nychka, and L. O. Mearns (2015). "A New Distribution Technique for Climate Model Bias Correction". Machine Learning and Data Mining Approaches to Climate Science: Proceedings of the 4^{th} International Workshop on Climate Informatics, 25-26 September 2015. Ed. V. Lakshmanan, E. Gilleland, A. McGovern, and M. Tingley. Switzerland: Springer International, 2015. 91-99.

Manka, B.N., J.M. Hathaway, R.A. Tirpak, Q. He, W.F. Hunt. (2016). "Driving forces of effluent nutrient variability in field scale bioretention." Ecological Engineering, 94, 622-628.
McGinnis, S. (2018). climod: Bias correction via KDDM (Kernel Density Distribution Mapping quantile mapping based on nonparametric PDF estimates) plus associated utilities for working with regional climate model (RCM) output in netcdf format. R package version 0.0.1.

Mearns, L.O., et al. (2017). The NA-CORDEX dataset, version 1.0. NCAR Climate Data Gateway, Boulder CO. Accessed April 2019. Available from: https://doi.org/10.5065/D6SJ1JCH.

Miller, R. (1978). The Hydraulically Effective Impervious Area of an Urban Basin. Broward County, Florida.

Minnesota Pollution Control Agency (MPCA) (2016). Design criteria for bioretention. St. Paul, Minnesota: MPCA.

Moore, T. L., J. S. Gulliver, L. Stack, and M. H. Simpson (2016). "Stormwater management and climate change: vulnerability and capacity for adaptation in urban and suburban contexts". Climatic Change, 138, 491-504.

Niazi, M., C. Nietch, M. Maghrebi, N. Jackson, B. R. Bennett, M. Tryby, and A. Massoudieh (2017). "Storm Water Management Model: Performance Review and Gap Analysis". Journal of Sustainable Water in the Built Environment, 3(2), 04017002.

North Carolina Department of Environmental Quality (NCDEQ) (2009). Stormwater BMP Manual: Bioretention. Raleigh, North Carolina: NCDEQ.

Olsson, J., K. Berggren, M. Olofsson, and M. Viklander (2009). "Applying climate model precipitation scenarios for urban hydrological assessment: a case study in Kalmar City, Sweden". Atmospheric Research, 92, 364-375.

Pyke, C., M. P. Warren, T. Johnson, J. LaGro Jr., J. Scharfenberg, P. Groth, R. Freed, W. Schroeer, and E. Main (2011). "Assessment of low impact development for managing stormwater with changing precipitation due to climate change". Landscape and Urban Planning, 103, 166-173.

R Core Team (2019). R: A language and environment for statistical computing. R Foundation for Statistical Computing, Vienna, Austria. Available from: https://www.R-project.org/.

Ramshani, M., A. Khojandi, X. Li, and O. Omitaomu (2020). "Optimal planning of the joint placement of photovoltaic panels and green roofs under climate change uncertainty". Omega, 90, 101986.

Read, J., T. Wevill, T. Fletcher, and A. Deletic (2008). "Variation among plant species in pollutant removal from stormwater biofiltration systems". Water Research, 42, 893-902.

Rosenberg, E. A., P. W. Keys, D. B. Booth, D. Hartley, J. Burkey, A. C. Steinemann, and D. P. Lettenmaier (2010). "Precipitation extremes and the impacts of climate change on stormwater infrastructure in Washington State". Climatic Change, 102, 319-349.

Rossman, L. A. (2015). Storm Water Management Model User's Manual Version 5.1. National Risk Management Research Laboratory, Office of Research and Development, U.S. Environmental Protection Agency, Cincinnati, OH.

Semadeni-Davis, A., C. Hernebring, G. Svensson, and L. G. Gustafsson (2008). "The impacts of climate change and urbanisation on drainage in Helsingborg, Sweden: Combined sewer system". Journal of Hydrology, 350, 110-113.

Stephens, G., T. L'Ecuyer, R. Forbes, A. Gettlemen, J. C. Golaz, A. Bodas-Salcedo, K. Suzuki, P. Gabriel, and J. Hayne (2010). "Dreary state of precipitation in global models". Journal of Geophysical Research, 2, D24211.

Sun, Y. and S. Solomon (2005). "How often does it rain?". Journal of Climate, 19, 917-934.

Tennessee Climatological Service (2018). "Climate Data for Tennessee". The University of Tennessee Institute of Agriculture. Retrieved on July 17, 2019 from: https://ag. tennessee.edu/climate/Pages/climatedataTN.aspx.

Tennessee Department of Environment and Conservation (TDEC) (2014). Tennessee Permanent Stormwater Management and Design Guidance Manual. Tennessee Department of Environment and Conservation, Division of Water Resources, Nashville, TN.

U.S. Global Change Research Program (USGCRP) (2018). Impacts, Risks, and Adaptation in the United States: Fourth National Climate Assessment, Volume II [Reidmiller, D.R., C.W. Avery, D.R. Easterling, K.E. Kunkel, K.L.M. Lewis, T.K. Maycock, and B.C. Stewart (eds.)]. Washington, DC, USA, 1515 pp. DOI: 10.7930/NCA4.2018.

Unidata Science Gateway (2020). Available at: science-gateway.unidata.ucar.edu. DOI: 10.5065/688s-2w73.

Walsh, C. J., A. H. Roy, J. W. Feminella, P. D. Cottingham, P. M. Groffman, and R. P. Morgan (2005). "The urban stream syndrome: current knowledge and the search for a cure". Journal of the North American Benthological Society, 24(3), 706-723.

Wang, M., D. Zhang, A. Adhityan, W. J. Ng, J. Dong, and S. K. Tan (2016). "Assessing cost-effectiveness of bioretention on stormwater in response to climate change and urbanization for future scenarios". Journal of Hydrology, 543, 423-432.

Wang, M., D. Q. Zhang, Y. Cheng, and S. K. Tan (2019a). "Assessing performance of porous pavements and bioretention cells for stormwater management in response to probable climatic changes". Journal of Environmental Management, 243, 157-167.

Wang, M., D. Zhang, S. Lou, Q. Hou, Y. Liu, Y. Cheng, J. Qi, and S. K. Tan (2019b). "Assessing hydrological effects of bioretention cells for urban stormwater runoff in response to climatic changes". Water, 11(5), 997.

Willems, P., K. Arnbjerg-Nielsen, J. Olsson, and V. T. V. Nguyen (2012). "Climate change impact assessment on urban rainfall extremes and urban drainage: Methods and shortcomings". Atmospheric Research, 103, 106-118.

Winston, R. J., J. D. Dorsey, and W. F. Hunt (2016). "Quantifying volume reduction and peak flow mitigation for three bioretention cells in clay soils in northeast Ohio". Science of the Total Environment, 553, 83-95.

Winston, R. J. (2016). "Resilience of green infrastructure under extreme conditions". Ph.D. dissertation, North Carolina State University, Raleigh, North Carolina, USA.

Zahmatkesh, Z., S. Burian, M. Karamouz, H. Tavakol-Davani, and E. Goharian (2014). "Low-impact development practices to mitigate climate change effects on urban stormwater runoff: case study of New York City". Journal of Irrigation and Drainage Engineering, 141(1), 04014043.

Zahmatkesh, Z., M. Karamouz, E. Goharian, and S. J. Burian (2015). "Analysis of the effects of climate change on urban storm water runoff using statistically downscaled precipitation data and a change factor approach". Journal of Hydrologic Engineering, 20(7), 05014022.

Zhang, K., D. Manuelpillai, B. Raut, A. Deletic, and P. M. Bach (2019). "Evaluating the reliability of stormwater treatment systems under various future climate conditions". Journal of Hydrology, 568, 57-66.